International Journal of Applied Mathematical Sciences
ISSN 0973-0176 Volume 9, Number 1 (2016), pp. 77-101

http://www.ripublication.com

Slip Velocity On A Casson Fluid Flow Over A Vertical Porous Surface With Heat Generation Or Absorption In A Non-Darcy Porous Medium

P. Sathies Kumar[1], M. Bharathi Devi[2] and K. Gangadhar[3]

[1]Department of Mathematics, Raghava Degree College, Ongole, A.P
[2]Department of Mathematics, RISE Group of Institutions, Ongole, A.P
[3]Department of Mathematics, Acharya Nagarjuna University,
Ongole, Andhra Pradesh-523001, India
Authors Email ID: satishpallas@gmail.com, mattabharathi@gmail.com,
kgangadharmaths@gmail.com

Abstract

This paper investigated a numerical solution to a chemically reacting and electrically conducting Casson fluid flow over a vertical porous surface in the presence of non-Darcy porous medium and slip velocity. Using the similarity transformations, the governing equations are transformed into a system of non linear ordinary differential equations. Using the fourth order Runge-Kutta Gill Procedure combined with shooting technique, the reduced system of equations are solved. The results are showed graphically and also tabulated for different controlling parameters. In comparisons with published results of the literature, the present numerical results are validated.

Keywords: Casson fluid, MHD, slip velocity, non-Darcy porous medium, heat generation or absorption.

1. Introduction

The fluid flow in the presence of a non-Darcy Porous medium is studied by a number of authors. Makanda et al. (2015) studied the effect of radiation upon magneto hydro dynamic free convection of a Casson fluid flow from a cylinder in a non-Darcy Porous medium with Partial slip flow. They concluded that with the increase of the velocity slip factor the resultant skin-friction coefficient is increased.. Siva Ram Prasad and Hemalatha (2016) analyzed the thermal radiation and melting effect on a MHD flow over a vertical plate embedded in Non-Newtonian fluid saturated non-Darcy Porous medium. Mahdy and Gorla (2014) studied the soret and dufour effects

on MHD non-Darcian natural convection from a vertical wavy surface embedded in a Porous medium. Murthy and Singh (2000) studied the thermal dispersion effects of thermal dispersion on non-Darcy convection over a cone. Srinivasacharya and Vijaykumar (2015) studied the mixed convection with radiation effect in a nanofluid along an inclined surface embedded in a non-Darcy Porous medium. Chamkha et al. (2010) observed an increase in the Nusselt number for both opposing and aiding external flows by increasing the heat generation or absorption parameter. The Nusselt number increased with the increase of the non-Darcy porous medium parameter for opposing external flow while it is decreased for aiding external flow. On a two dimensional boundary layer flow of an incompressible Casson fluid in a Porous medium, the effects of magneto hydro dynamics (MHD) and a heat absorption or heat generation is studied by Shehzad et al. (2016).

Many studies are conducted a fluid flow Past a vertical geometry. Aly et al. (2003) observed the existence and uniqueness of a vertically flowing fluid passed a model of a thin vertical fin in a saturated porous media. Bhattacharya et al. (2013) investigated the mixed convective boundary layer slip flow over a vertical plate. Gorla and Chamkha (2011) studied the non-isothermal vertical plate embedded in a porous medium saturated with a nanofluid. Aman and Ishak (2012) investigated the mixed convection flow towards an impermeable vertical plate with a boundary surface condition. Siddiqa and Hossain (2012) observed the mixed convective boundary layer flow of a viscous fluid along a heated vertical plate.. Heat transfer characteristics of steady mixed convection flow over a permeable vertical flat plate embedded in an isothernal fluid saturated porous medium is studied by Bachok et al. (2010).To give a mathematical model for the system to predict the reactor performance the field of chemical reaction analysis is the trend at present. Much amount of research work has been reported in this field. Particularly the study of heat and mass transfer with chemical reaction is of great importance in chemical and hydrometallurgical industries. Chemical reaction can be coded as either heterogeneous or homogeneous processes. This depends on either they occur an interface or as a single phase volume reaction. Seta et al. (2016) found that chemical reaction tends to reduce species concentration whereas diffusion has a reverse effection it. Also chemical reaction tends to increase the rate of mass transfer on the plate whereas mass diffusion has a reverse effect on it. Also, chemical reaction tends to increase the rate of mass transfer on the plate whereas mass diffusion has a reverse effect on it. Abbas et al. (2016) observed the diffusion of chemically reacting species on a porous plate of a third grade flow. Mythili et al. (2015) concluded that the increase in the order of chemical reaction parameter results in retarding effect in concentration distribution. Hayal et al. (2015) studied the effect of temperature and concentration stratification in a mixed convection flow of an oldroyd-B fluid with thermal radiation and chemical reaction. Gangadhar et al. (2012) concluded that local skin friction coefficient, local heat and mass transfer rate on the plate surface increased the intensity of chemical reaction parameter.

The studies invariably assumed the ‘no-slip’ condition at the boundary. However, the slip effects are shown to be significant in same of industrial thermal problems and manufacturing third dynamic systems, Uddin et al. (2014) concluded that

hydrodynamic (momentum) is slip increase is significantly retards the boundary layer flow as it markedly increases the temperature and nanoparticle concentration values. Subbarao et al. (2015) found that by increasing slip velocity, the temperature throughout the boundary layer region is consistently enhanced..But the increasing slip velocity induces acceleration in the flow near the surface of the sphere with the reverse effect from the surface. Shaw et al. (2016) revealed that thermal slip coefficient reduces the momentum and thickness of thermal boundary layer.

This paper investigated a numerical solution to an electrically conducting and chemically reacting Casson fluid flow past a vertical porous surface in the presence of non-darcy porous medium and slip velocity. By using the similarity transformations, the governing equations are transformed a system of non linear ordinary differential equations. Using the fourth order Runge-Kutta Gill procedure with shooting technique, the reduced system of equations is solved. The results are shown graphically and are tabulated for various controlling parameters. The numerical results are validated in comparison with already published results in literature.

2. MATHEMATICAL FORMULATION

Consider a two dimensional steady incompressible, electrically conducting and chemically reacting Casson fluid flow past a vertical porous stretching surface in a non-Darcy porous medium. The schematic diagram and coordinate system is shown in figure A. let the x-axis be taken along the direction of the plate and y-axis normal to it. The fluid occupies the half space y>0. The influence of heat generation or absorption is considered on right hand side of the energy equation. The mass transfer phenomenon with chemical reaction is also retained. The flow is subjected to a constant applied magnetic field B_o in the y direction. The magnetic Reynolds number is considered to be very small so that the induced magnetic field is negligible is comparison to the applied magnetic field. The schematic diagram and coordinate system of the problem is shown in figure A.

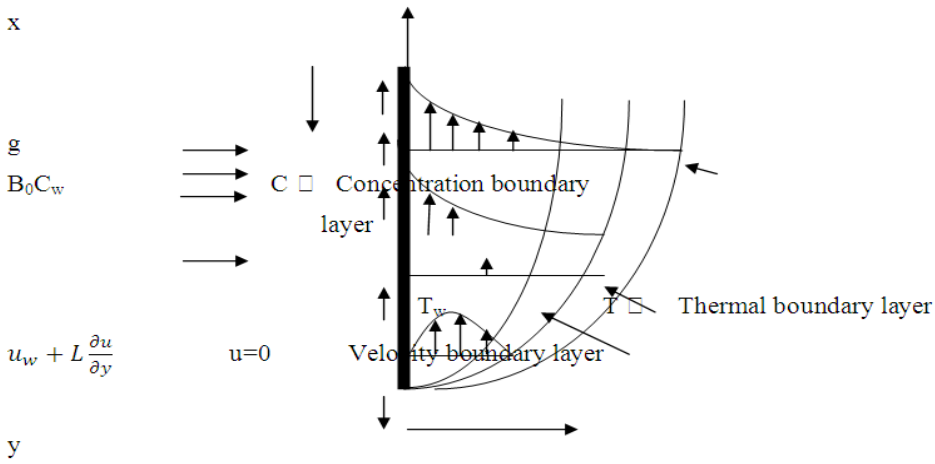

Figure A: Schematic diagram and coordinate system of the physical problem

The rheological equation of state for an isotropic flow of a Casson fluid (Eldabe and Salwa (1995)) can be expressed as

$$\tau_{ij} = \begin{cases} \left(\mu_B + \frac{p_y}{\sqrt{2\pi}}\right) 2e_{ij}, & \pi > \pi_c \\ \left(\mu_B + \frac{p_y}{\sqrt{2\pi_c}}\right) 2e_{ij}, & \pi < \pi_c \end{cases} \tag{2.1}$$

where $\mu_B$is plastic dynamic viscosity of the non-Newtonian fluid, $p_y$is the yield stress of fluid, $\pi$is the product of the component of deformation rate with itself, namely, $\pi = e_{ij}e_{ij}$, $e_{ij}$is the $(i, j)^{th}$ component of the deformation rate, and $\pi_c$is critical value of πbased on non-Newtonian model.

The governing equations of continuity, momentum, energy and species are written as bellow with the Boussinesq and the boundary layer approximations.

Continuity equation

$$\frac{\partial u}{\partial x} + \frac{\partial v}{\partial y} = 0 \tag{2.2}$$

Momentum equation

$$u\frac{\partial u}{\partial x} + v\frac{\partial u}{\partial y} = \upsilon\left(1 + \frac{1}{\beta}\right)\frac{\partial^2 u}{\partial y^2} + g\beta_T\left(T - T_\infty\right) + g\beta_C\left(C - C_\infty\right) - \frac{\sigma B_0^2}{\rho}u - \frac{\upsilon}{k'}u - \frac{b}{k'}u^2 \tag{2.3}$$

Energy equation

$$u\frac{\partial T}{\partial x} + v\frac{\partial T}{\partial y} = \alpha\frac{\partial^2 T}{\partial y^2} + \frac{Q_0}{\rho c_p}(T - T_\infty) \tag{2.4}$$

Species equation

$$u\frac{\partial C}{\partial x} + v\frac{\partial C}{\partial y} = D_m\frac{\partial^2 C}{\partial y^2} - k_0(C - C_\infty) \tag{2.5}$$

The boundary conditions for the velocity, temperature and concentration fields are

$$u = u_w + L\upsilon\frac{\partial u}{\partial y}, v = -v_0, T = T_w, C = C_w \text{ at } y = 0 \tag{2.6}$$

$$u \to 0, T \to T_\infty, C \to C_\infty \text{ as } y \to \infty \tag{2.7}$$

Where u and v are the velocity component along the x and y axes respectively, $\beta = \mu_B\sqrt{2\pi_c} / P_y$ is the non-Newtonian Casson fluid parameter, υ is the kinematic viscosity of the fluid, k′ is the permeability of the porous medium, b is the Forchheimer constant, v_0 is the suction velocity from the surface, α is the thermal diffusivity, D_m is the mass diffusivity, T is the temperature of the fluid, T_w is the temperature at the surface, T_∞ is the free stream temperature, Q_0 is the heat source or sink constant, C is the concentration of the fluid, C_w is the concentration at the surface, C_∞ is the free stream concentration, β_T is the thermal expansion coefficient, β_c is the solutal expansion coefficient, ρ is the fluid density, g is gravitational acceleration, k_0 is the chemical reaction rate constant, L is the initial value of the velocity slip factor and σ *is* electrical conductivity.

The equation of continuity is satisfied for the choice of a stream function ψ (x, y) such that

$$u = \frac{\partial \psi}{\partial y} \text{ and } v = -\frac{\partial \psi}{\partial x} \tag{2.8}$$

Now, we are introducing the following similarity transformations

$$\eta = y\sqrt{\frac{u_w}{\upsilon x}}, \psi(\eta) = \sqrt{u_w \upsilon x} f(\eta) \tag{2.9}$$

Where $\upsilon = \frac{\mu}{\rho}$ is the kinematic viscosity

$f(\eta) = \frac{\psi(\eta)}{\sqrt{u_w \upsilon x}}$ is the dimensionless stream function

The dimensionless temperature and concentration are

$$\theta(\eta) = \frac{T - T_\infty}{T_w - T_\infty} \tag{2.10}$$

$$\phi(\eta) = \frac{C - C_\infty}{C_w - C_\infty} \tag{2.11}$$

After the substitution of these transformations (2.8) – (2.11) along with the boundary conditions (2.6) and (2.7) in the equations (2.3) – (2.5), the resulting non-linear ordinary differential equations are written as follows:

$$\left(1 + \frac{1}{\beta}\right) f'''(\eta) + f(\eta) f''(\eta) + Gr\theta(\eta) + Gc\phi(\eta) - \left(M + f'(\eta)\right) f'(\eta) - \frac{1}{Da \operatorname{Re}_x} f'(\eta) - \frac{Fs}{Da} f'(\eta)^2 = 0 \tag{2.12}$$

$$\frac{1}{\Pr}\theta''(\eta) + f(\eta)\theta'(\eta) + Q\theta(\eta) = 0 \tag{2.13}$$

$$\frac{1}{Sc}\phi''(\eta) + f(\eta)\phi'(\eta) - Kr\phi(\eta) = 0 \tag{2.14}$$

The corresponding boundary conditions are

$$f(0) = f_w, f'(0) = 1 + \lambda f''(0), \theta(0) = 1, \phi(0) = 1$$

$$f' = \theta = \phi = 0 \text{ as } \eta \to \infty \tag{2.15}$$

where the primes denote differentiation with respect to η

the dimensionless numbers in the above transformed equations are the local Darcy number (Da), Forchheimer number (Fs), Reynolds number (Re_x), thermal Grashof number (Gr), solutal Grashof number (Gc), Prandtl number (Pr) and Schmidt number (Sc) which are defined as follows

$$Da = \frac{k'}{x^2},\ Fs = b/x,\ \operatorname{Re}_x = \frac{ax^2}{\upsilon},\ \Pr = \frac{\upsilon}{\alpha},$$

$$Gr = \frac{g\beta_T (T_w - T_\infty) x}{u_w^2},\ Gc = \frac{g\beta_c (C_w - C_\infty) x}{u_w^2}$$

$$Sc = \frac{\upsilon}{D_m}$$

Moreover, $M = \frac{\sigma B_0^2}{a\rho}$ is the magnetic field parameter, $f_w = -\frac{v_0(x)}{\sqrt{a\upsilon}}$ is the suction (>0) or the injection (<0) parameter, $\lambda = L\sqrt{\frac{a}{\upsilon}}$ is the slip parameter, $Kr = \frac{k_0}{a}$ is the chemical reaction parameter and $Q = \frac{Q_0}{a\rho c_p}$ is the heat generation (>0) or absorption (<0) parameter.

The parameters of significant interest for the present problem are the skin-friction coefficient C_{fx}, local Nusselt number Nu_x and local Sherwood number Sh_x which are given by

$$C_{fx} = \frac{\tau_w}{\rho u_w^{\,2}},\ Nu_x = \frac{xq_w}{k\left(T_w - T_\infty\right)},\ Sh_x = \frac{xq_m}{D_m(C_w - C_\infty)} \tag{2.16}$$

Where the local wall shear stress τ_w, the heat transfer from the surface q_w and the mass transfer from the surface q_m are defined by

$$\tau_w = -\mu_B\left(1+\frac{1}{\beta}\right)\left(\frac{\partial u}{\partial y}\right)_{y=0},\ q_w = -k\left(\frac{\partial T}{\partial y}\right)_{y=0}$$

$$q_m = -D_m\left(\frac{\partial C}{\partial y}\right)_{y=0} \tag{2.17}$$

Using the similarity variables (2.8) – (2.11), the resulting equations are

$$C_{fx}\,\mathrm{Re}_x^{1/2} = -\left(1+\frac{1}{\beta}\right)f''(0)$$

$$Nu_x\,\mathrm{Re}_x^{\,-1/2} = -\theta'(0) \tag{2.18}$$

$$Sh_x\,\mathrm{Re}_x^{-1/2} = -\phi'(0)$$

Where $\mathrm{Re}_x = \frac{u_w x}{\upsilon}$ is the local Reynolds number.

3 SOLUTION OF THE PROBLEM

The set of equations (2.12) to (2.15) were reduced to a system of first-order differential equations and solved using a MATLAB boundary value problem solver called **bvp4c**. By implementing a collocation method subject to general nonlinear, two-point boundary conditions $g\left(y(a), y(b), p\right)$, this program solves boundary value problems for ordinary differential equations of the form $y' = f\left(x, y, p\right), a \le x \le b$, Here ***p***is a vector of unknown parameters. Boundary value problems (BVPs) arise in most diverse forms. Just about any BVP can be formulated for solution with **bvp4c**.

The first step is to write the *ODEs* as a system of first order ordinary differential equations. The details of the solution method are presented in Shampine and Kierzenka (2000).

4 RESULTS AND DISCUSSION

The governing equations (2.12)-(2.14) subject to the boundary conditions (2.15) are integrated as described in section 3. In order to get a clear insight of the physical problem, the velocity, temperature and concentration have been discussed by assigning numerical values to the parameters encountered in the problem.

In order to verify the accuracy of our present results, comparisons have been made with the available results of Arthur et al. (2015), Shezad et al. (2013), Salem and El Aziz (2008), Anderson et al. (1994) in the literature which are shown in table 1 relating to local Sherwood Number $(-\phi'(0))$ for different values of Casson fluid parameter (β) and Schmidtnumber (Sc) with M=λ=Gr =Gc =Pr=Fs= Q =0 as $\beta \to \infty, Re_x \to \infty$. Also comparisons have been made with the available results of Arthur et al. (2015) in the literature, which are demonstrated in table 2 relating to local Skin-Friction coefficient $(-f''(0))$ and local Sherwood number $(-\phi'(0))$ for different values of Magnetic parameter (M), Casson fluid Parameter (β), solutal Grashof number (Gc), Schmidt number (Sc), chemical reaction parameter (Kr) and suction parameter (fw) for fixed Pr= Q =λ=Fs=Gr=0 as $Re_x \to \infty$. It is eatablished that the results obtained in the present work shows a good agreement with the previously published results.

Figures 1a-1c depicts the effect of magnetic parameter (M) in dimensionless velocity, temperature and concentration distributions respectively. The effect of magnetic parameter is explicated by setting the values of the other parameters to be constant for β = 0.5, Re_x = 1, Gr = 0.2, Gc = 0.2, Fs = 0.1, Da = 0.2, Pr = 2, Q = 0.3, Sc = 0.24, kr = 0.3, λ = 0.4 & f_w = 0.5. It is seen that the dimensionless velocity distribution of the fluid decreases with an increasing the magnetic parameter (see figure1a). The magnetic parameter is found to retard the velocity at all points of the flow field. It is because that the application of transverse magnetic field will result in a resistive type force (Lorentz force) similar to drag force which tends to resist the fluid flow and thus reducing its velocity. The dimensionless temperature and concentration distribution of the fluid increases throughout the boundary layer with raising the magnetic parameter (figure 1b &1c).

Figures 2a-2c shows that the effect of non-Newtonian Casson parameter (β) on dimensionless velocity, temperature and concentration distributions respectively. The other parameters are set constantly atM = 0.5, Re_x = 1, Gr = 0.2, Gc = 0.2, Fs = 0.1, Da = 0.2, Pr = 2, Q = 0.3, Sc = 0.24, kr = 0.3, λ = 0.4 & f_w = 0.5. It is observed that dimensionless velocitydistribution of the fluid decreases with an increasing the values of non-Newtonian Casson parameter (Figures 2a).Thedimensionless temperature and concentration distribution of the fluid increases with the influence of non-Newtonian Casson parameter (Figure 2b & 2c).

Figures 3a-3c depicts that the effect of Reynolds number (Re_x) on dimensionless velocity, temperature and concentration distributions respectively. The other

parameters are set constantly at M = 0.5, β = 0.5, Gr = 0.2, Gc = 0.2, Fs = 0.1, Da = 0.2, Pr = 2, Q = 0.3, Sc = 0.24, kr = 0.3, λ = 0.4 & f_w = 0.5. $Re_x$is defined as the ratio of inertial forces to viscous forces.It is observed that dimensionless velocity distribution of the fluid increases with an increasing the values of Reynolds number (Figures 3a). The dimensionless temperature and concentration distribution of the fluid increases with the influence of Reynolds number (Figure 3b & 3c).

Figures 4a-4c depicts that the effect of local thermal Grashof number (Gr) on dimensionless velocity, temperature and concentration distributions respectively. The other parameters are set constantly at M = 0.5, β = 0.5, Re_x = 1, Gc = 0.2, Fs = 0.1, Da = 0.2, Pr = 2, Q = 0.3, Sc = 0.24, kr = 0.3, λ = 0.4 & f_w = 0.5. It is observed that dimensionless velocity distribution of the fluid increases with an increasing the values of local thermal Grashof number (Figures 4a). The dimensionless temperature and concentration distribution of the fluid decreases with the influence of Grash number (Figure 4b &4c).

Figures 5a-5c depicts that the effect of local solutal Grashof number (Gc) on dimensionless velocity, temperature and concentration distributions respectively. The other parameters are set constantly at M = 0.5, β = 0.5, Re_x = 1, Gr = 0.2, Fs = 0.1, Da = 0.2, Pr = 2, Q = 0.3, Sc = 0.24, kr = 0.3, λ = 0.4 & f_w = 0.5. It is observed that dimensionless velocity distribution of the fluid increases with an increasing the values of local solutal Grashof number (Figures 5a). The dimensionless temperature and concentration distribution of the fluid decreases with the influence of local solutal Grashof number (Figure 5b & 5c).

Figures 6a-6c depicts that the effect of Darcy number (Da) on dimensionless velocity, temperature and concentration distributions respectively. The other parameters are set constantly at M = 0.5, β = 0.5, Re_x = 1, Gr = 0.2, Gc = 0.2, Fs = 0.1, Pr = 2, Q = 0.3, Sc = 0.24, kr = 0.3, λ = 0.4 & f_w = 0.5. It is observed that dimensionless velocity distribution of the fluid increases with an increasing the values of Darcy number (Figures 4a). The dimensionless temperature and concentration distribution of the fluid decreases with the influence of Darcy number (Figure 6b & 6c).

Figures 7a-7c depicts that the effect of Forchheimer number (Fs) on dimensionless velocity, temperature and concentration distributions respectively. The other parameters are set constantly at M = 0.5, β = 0.5, Re_x = 1, Gr = 0.2, Gc = 0.2, Da = 0.2, Pr = 2, Q = 0.3, Sc = 0.24, kr = 0.3, λ = 0.4 & f_w = 0.5. It is observed that dimensionless velocity distribution of the fluid decreases with an increasing the values of Forchheimer number (Figure 7a). The dimensionless temperature and concentration distribution of the fluid increases with the influence of Forchheimer number (Figure 7b &7c).

Figures 8a-8c depicts that the effect of suction or injection parameter (fw) on dimensionless velocity, temperature and concentration distributions respectively. The other parameters are set constantly at M = 0.5, β = 0.5, Re_x = 1, Gr = 0.2, Gc = 0.2, Fs = 0.1, Da = 0.2, Pr = 2, Q = 0.3, Sc = 0.24, kr = 0.3 & λ = 0.4. It is observed that dimensionless velocity distribution of the fluid decreases with an increasing the values of suction or injection parameter (Figures 8a). The dimensionless temperature and concentration distribution of the fluid decreases with the influence of suction or injection parameter (Figure 8b & 8c).

Figures 9a-9c depicts that the effect of velocity slip parameter (λ) on dimensionless velocity, temperature and concentration distributions respectively. The other parameters are set constantly at M = 0.5, β = 0.5, Re_x = 1, Gr = 0.2, Gc = 0.2, Fs = 0.1, Da = 0.2, Pr = 2, Q = 0.3, Sc = 0.24, kr = 0.3 & f_w = 0.5. It is observed that dimensionless velocity distribution of the fluid decreases with an increasing the values of velocity slip parameter (Figures 9a). The dimensionless temperature and concentration distribution of the fluid increases with the influence of velocity slip parameter (Figure 9b & 9c).

Setting the other parameters to be constants as M = 0.5, β = 0.5, Re_x = 1, Gr = 0.2, Gc = 0.2, Fs = 0.1, Da = 0.2, Q = 0.3, Sc = 0.24, kr = 0.3, λ = 0.4 & f_w = 0.5. Figure 10 shows that the effect of Prandtl number (Pr) on dimensionless temperature. It can be observed that the dimensionless temperature is decreased on increasing Prandtl number. Physically, increasing Prandtl number becomes a key factor to reduce the thickness of the thermal boundary layer

For the constant parametersM = 0.5, β = 0.5, Re_x = 1, Gr = 0.2, Gc = 0.2, Fs = 0.1, Da = 0.2, Pr = 2, Sc = 0.24, kr = 0.3, λ = 0.4 & f_w = 0.5. The effect of heat source (Q > 0) or sink parameter (Q < 0) on the temperature is plotted in Figure 11. It can be showed that the effect of heat absorption results in a fall of temperature since heat resulting from the wall is absorbed. Obviously, the heat generation leads to an increase in temperature throughout the entire boundary layer. Furthermore, it should be noted that for the case of heat generation, the fluid temperature become maximum in the fluid layer adjacent to the wall rather at the wall. In fact, the heat generation effect not only has the tendency to increase the fluid temperature but also increase the thermal boundary layer thickness. Due to heat absorption, it is observed that the fluid temperature as well as the thermal boundary layer thickness is decreased. No significance in heat distribution is observed among the fluids in the presence of heat absorption.

Setting the other parameters to be constants as M = 0.5, β = 0.5, Re_x = 1, Gr = 0.2, Gc = 0.2, Fs = 0.1, Da = 0.2, Pr = 2, Q = 0.3, kr = 0.3, λ = 0.4 & f_w = 0.5. Figure 12 shows that the effect of Schmidt number (Sc) on dimensionless concentration distribution. It can be observed that the dimensionless concentration distribution is decreased on increasing Schmidt number.

Setting the other parameters to be constants as M = 0.5, β = 0.5, Re_x = 1, Gr = 0.2, Gc = 0.2, Fs = 0.1, Da = 0.2, Pr = 2, Q = 0.3, Sc = 0.24, λ = 0.4 & f_w = 0.5. Figure 13 shows that the effect of chemical reaction parameter (kr) on dimensionless concentration distribution. It can be observed that the dimensionless concentration distribution is decreased on increasing chemical reaction parameter.

The effects of the magnetic parameter (M), non-Newtonian Casson parameter (β), Reynolds number (Re_x), local thermal Grashof number (Gr), local solutal Grashof number (Gc), Darcy number (Da) and Forchheimer number (Fs) on the skin-friction coefficient $-f''(0)$, local Nusselt number $-\theta'(0)$ and local Sherwood number $-\phi'(0)$ are illustrated in Table 3 by choosing the other parameters constantly atPr = 2, Q = 0.3, Sc = 0.24, kr = 0.3, λ = 0.4 & f_w = 0.5. On increasing the values of magnetic parameter, non-Newtonian Casson parameter andForchheimer number then the resultant skin friction coefficient is increased but local Nusselt number and local

Sherwood number are decreased.The skin friction coefficient is decreased whereas the local Nusselt number and local Sherwood number are increased by increasing the values of Reynolds number, local thermal Grashof number, local solutal Grashof number and Darcy number.

By varying the values of Prandtl number (Pr), heat generation (Q>0) or heat absorption (Q<0) parameter, Schmidt number (Sc), chemical reaction parameter (kr), velocity slip parameter (λ) and suction ($f_w > 0$) or injection ($f_w < 0$) parameter on the skin-friction coefficient $-f''(0)$, local Nusselt number $-\theta'(0)$ and local Sherwood number $-\phi'(0)$ are illustrated in Table 4.Setting the other parameters to be constants as M = 0.5, β = 0.5, Re_x = 1, Gr = 0.2, Gc = 0.2, Fs = 0.1 & Da = 0.2.By increasing the values of Prandtl number the skin friction coefficient and local Nusselt number are increased whereas local Sherwood number is decreased. On increasing the values of heat generation or heat absorption parameter the resultant skin friction coefficient and local Nusselt number are decreased whereas local Sherwood number is increased. The local shin friction coefficient and local Sherwood number increases whereas the local Nusselt number decreases on increasing the Schmidt number and chemical reaction parameter. With the influence of velocity slip parameter, the skin friction coefficient, the local Nusselt number and local Sherwood numbers are decreased. The skin friction coefficient, the local Nusselt number and local Sherwood numbers are increased by increasing the values of suction or injection parameter.

5 CONCLUSIONS

This paper investigated a numerical solution to an electrically conducting and chemically reacting Casson fluid flow past a vertical porous surface in the presence of non-Darcy porous medium and slip velocity. The governing equations are approximated to a system of non-linear ordinary differential equations by similarity transformation. Numerical calculations are carried out for various values of the dimensionless parameters of the problem. It has been found that

1. The increase in the values of the magnetic parameter leads to a significant decrease in flow velocity and a significant increase in flow temperature and concentration profiles.
2. On increasing the values of Casson fluid parameter, a decrease is observed in flow velocity whereas the flow temperature and concentration is increased.
3. When the thermal Grashof number and solutal Grashof number increases, the resultant flow velocity increased. Thickness thermal and concentration boundary layers significantly decrease away from the surface when the thermal Grashof number and solutal Grashof number increases.
4. When the Darcy number increases, the viscous boundary layer thickness considerably increase whereas temperature and concentration boundary layer thickness is decreased and quiet opposite results were found in the presence of Forchheimer number.
5. The temperature distribution across the surface in the presence of heat generation is more significantly higher than in the absence of the heat generation.

6. When the slip parameter is imposed, the flow velocity decreases but thicknesses of the thermal and concentration boundary layers are increased.
7. Increasing the slip parameter strictly decreases the values of local skin friction coefficient, Nusselt and Sherwood numbers.
8. The heat and mass transfer rates increase rapidly on increasing the buoyancy parameters.
9. Increasing the Casson fluid parameter strictly increases the values of local skin friction coefficient while heat and mass transfer rates decrease.

Table 1: Comparison of local Sherwood number $-\phi'(0)$ with the available results in literature for different values of β and Sc with M = λ = Gr = Gc = Pr = Fs = Q = 0 as $\beta \to \infty, Re_x \to \infty$.

β	Sc	$-\phi'(0)$				
		Present study	Arthur et al. (2015)	Shezad et al. (2013)	Salem and El-Aziz (2008)	Anderson et al. (1994)
0.01	1.0	0.591355	0.591382	0.59136	0.592	0.59157
0.10	1.0	0.668980	0.668983	0.66898	0.669	0.66902
1.00	1.0	1.176500	1.176499	1.17650	1.177	1.17649
10.00	1.0	3.231228	3.231228	3.23175	3.232	3.23122

Table 2: Comparison of Skin friction coefficient $-f''(0)$ and local Sherwood number $-\phi'(0)$ with the available results in literature for different values of M, β, Gc, kr, f_w and Sc with Pr = Q = λ = Fs = Gr =0 as $Re_x \to \infty$.

M	β	Gc	Sc	kr	fw	$-f''(0)$		$-\phi'(0)$	
						Present study	Arthur et al. (2015)	Present study	Arthur et al. (2015)
0.5	0.5	0.1	0.6	0.3	0.1	0.701868	0.701894	0.675769	0.675765
0.7	0.5	0.1	0.6	0.3	0.1	0.747855	0.747866	0.670525	0.670528
1.0	0.5	0.1	0.6	0.3	0.1	0.812072	0.812075	0.663467	0.663476
1.5	0.5	0.1	0.6	0.3	0.1	0.909245	0.909246	0.653371	0.653385
0.5	0.3	0.1	0.6	0.3	0.1	0.584030	0.584131	0.690120	0.690091
0.5	1.5	0.1	0.6	0.3	0.1	0.942479	0.942483	0.650243	0.650258
0.5	2.0	0.1	0.6	0.3	0.1	0.993801	0.993805	0.645441	0.645458
0.5	0.5	0.5	0.6	0.3	0.1	0.615563	0.615589	0.684493	0.684487
0.5	0.5	1.0	0.6	0.3	0.1	0.511616	0.511641	0.694310	0.694304
0.5	0.5	1.0	0.6	0.3	0.1	0.411176	0.411199	0.703209	0.703204
0.5	0.5	0.1	0.5	0.3	0.1	0.700293	0.700321	0.607026	0.607036
0.5	0.5	0.1	1.0	0.3	0.1	0.705933	0.705957	0.911676	0.911669
0.5	0.5	0.1	1.5	0.3	0.1	0.708767	0.708792	1.155171	1.155165
0.5	0.5	0.1	0.6	0.5	0.1	0.703159	0.703184	0.764955	0.764950
0.5	0.5	0.1	0.6	1.0	0.1	0.705396	0.705420	0.949752	0.949749
0.5	0.5	0.1	0.6	1.5	0.1	0.706903	0.706927	1.102399	1.102396

0.5	0.5	0.1	0.6	0.3	0.5	0.774622	0.774640	0.831440	0.831437
0.5	0.5	0.1	0.6	0.3	1.0	0.874212	0.874223	1.04788	1.047186
0.5	0.5	0.1	0.6	0.3	1.5	0.982763	0.982768	1.281484	1.281483

Table 3 Numerical results for skin friction coefficient $-f''(0)$, local Nusselt number $-\theta'(0)$ and local Sherwood number $-\phi'(0)$ for M, β, Re_x, Gr, Gc, Da and Fs with Pr=2, Q = 0.3, Sc = 0.24, kr = 0.3, λ = 0.4 & f_w = 0.5.

M	β	Re_x	Gr	Gc	Da	Fs	$-f''(0)$	$-\theta'(0)$	$-\phi'(0)$
0	0.5	1	0.2	0.2	0.2	0.1	2.668585	1.04407	0.387600
0.5	0.5	1	0.2	0.2	0.2	0.1	2.739344	1.04077	0.387680
1	0.5	1	0.2	0.2	0.2	0.1	2.805567	0.996801	0.383364
1.5	0.5	1	0.2	0.2	0.2	0.1	2.867790	0.973952	0.381517
0.5	1	1	0.2	0.2	0.2	0.1	2.060645	0.894976	0.376267
0.5	1.5	1	0.2	0.2	0.2	0.1	1.807439	0.828803	0.370805
0.5	2	1	0.2	0.2	0.2	0.1	1.674057	0.786722	0.370804
0.5	0.5	2	0.2	0.2	0.2	0.1	1.764385	1.149147	0.399891
0.5	0.5	3	0.2	0.2	0.2	0.1	1.629082	1.199724	0.407444
0.5	0.5	4	0.2	0.2	0.2	0.1	1.550285	1.227324	0.412122
0.5	0.5	1	0.5	0.2	0.2	0.1	1.695877	1.043075	0.387495
0.5	0.5	1	1	0.2	0.2	0.1	1.586505	1.076754	0.390774
0.5	0.5	1	1.5	0.2	0.2	0.1	1.481886	1.106288	0.393841
0.5	0.5	1	0.2	0.5	0.2	0.1	1.593448	1.065324	0.390645
0.5	0.5	1	0.2	1	0.2	0.1	1.427530	1.125932	0.398983
0.5	0.5	1	0.2	1.5	0.2	0.1	1.267314	1.175645	0.406855
0.5	0.5	1	0.2	0.2	0.6	0.1	1.212856	1.208049	0.408575
0.5	0.5	1	0.2	0.2	0.8	0.1	1.148743	1.237690	0.413676
0.5	0.5	1	0.2	0.2	1	0.1	1.107614	1.256647	0.417180
0.5	0.5	1	0.2	0.2	0.2	0.3	1.256904	1.005724	0.384225
0.5	0.5	1	0.2	0.2	0.2	0.5	1.297788	0.992059	0.383148
0.5	0.5	1	0.2	0.2	0.2	0.8	1.354082	0.972749	0.381685

Table 3: Numerical results for skin friction coefficient $-f''(0)$, local Nusselt number $-\theta'(0)$ and local Sherwood number $-\phi'(0)$ for M, β, Re_x, Gr, Gc, Da and Fs with Pr = 2, Q = 0.3, Sc = 0.24, kr = 0.3, λ = 0.4 & f_w = 0.5.

Pr	Q	Sc	Kr	λ	f_w	$-f''(0)$	$-\theta'(0)$	$-\phi'(0)$
5	0.3	0.24	0.3	0.4	0.5	1.307335	2.727630	0.384462
10	0.3	0.24	0.3	0.4	0.5	1.333857	5.356732	0.384185
100	0.3	0.24	0.3	0.4	0.5	1.370451	50.602637	0.383956
2	-0.5	0.24	0.3	0.4	0.5	1.279774	1.861293	0.384185
2	-0.2	0.24	0.3	0.4	0.5	1.273357	1.620066	0.384937
2	0	0.24	0.3	0.4	0.5	1.267942	1.425737	0.385057
2	0.1	0.24	0.3	0.4	0.5	1.264741	1.311963	0.385139

2	0.2	0.24	0.3	0.4	0.5	1.261103	1.180549	0.385246
2	0.3	0.62	0.3	0.4	0.5	1.308858	1.009342	0.727632
2	0.3	0.78	0.3	0.4	0.5	1.322188	1.006515	0.854261
2	0.3	2.62	0.3	0.4	0.5	1.387758	0.993601	2.091904
2	0.3	0.24	0.5	0.4	0.5	1.266934	1.017614	0.455663
2	0.3	0.24	1	0.4	0.5	1.284491	1.013482	0.590011
2	0.3	0.24	1.5	0.4	0.5	1.296591	1.010764	0.695416
2	0.3	0.24	0.3	0.8	0.5	0.915235	0.853368	0.374283
2	0.3	0.24	0.3	1.2	0.5	0.721675	0.724598	0.368051
2	0.3	0.24	0.3	1.6	0.5	0.596396	0.610305	0.364111
2	0.3	0.24	0.3	0.4	-0.5	0.925551	-3.949705	0.280298
2	0.3	0.24	0.3	0.4	-0.2	1.028312	-3.645444	0.306851
2	0.3	0.24	0.3	0.4	0	1.096267	-2.308910	0.324864
2	0.3	0.24	0.3	0.4	0.2	1.162028	-0.144940	0.344072
2	0.3	0.24	0.3	0.4	0.5	1.256904	1.020134	0.385398

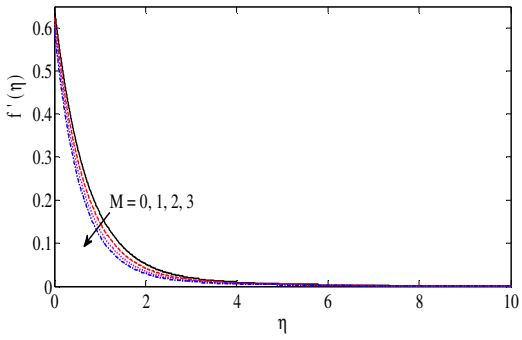

Figure 1a: Dimensionless velocitydistribution for different values of*M* with β = 0.5, Re_x = 1, Gr = 0.2, Gc = 0.2, Fs = 0.1, Da = 0.2, Pr = 2, Q = 0.3, Sc = 0.24, kr = 0.3, λ = 0.4 & f_w = 0.5.

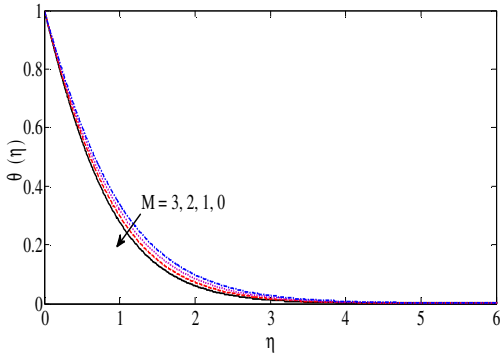

Figure 1b: Dimensionless temperature distribution for different values of *M*with β = 0.5, Re_x = 1, Gr = 0.2, Gc = 0.2, Fs = 0.1, Da = 0.2, Pr = 2, Q = 0.3, Sc = 0.24, kr = 0.3, λ = 0.4 & f_w = 0.5.

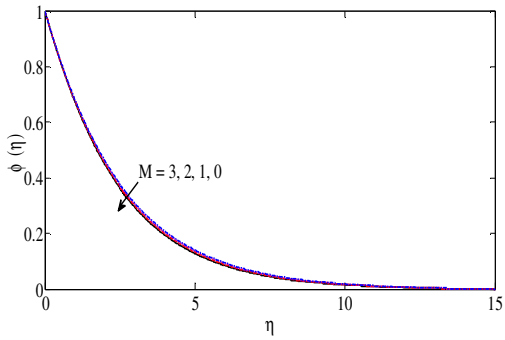

Figure 1c: Dimensionless concentration distribution for different values of *M* with β = 0.5, Re_x = 1, Gr = 0.2, Gc = 0.2, Fs = 0.1, Da = 0.2, Pr = 2, Q = 0.3, Sc = 0.24, kr = 0.3, λ = 0.4 & f_w = 0.5.

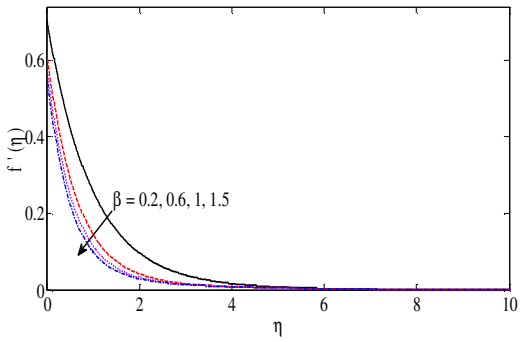

Figure 2a: Dimensionless velocity distribution for different values of*β* with M = 0.5, Re_x = 1, Gr = 0.2, Gc = 0.2, Fs = 0.1, Da = 0.2, Pr = 2, Q = 0.3, Sc = 0.24, kr = 0.3, λ = 0.4 & f_w = 0.5.

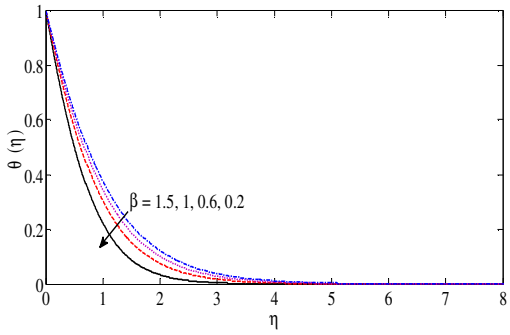

Figure 2b: Dimensionless temperature distribution for different values of*β* with M = 0.5, Re_x = 1, Gr = 0.2, Gc = 0.2, Fs = 0.1, Da = 0.2, Pr = 2, Q = 0.3, Sc = 0.24, kr = 0.3, λ = 0.4 & f_w = 0.5.

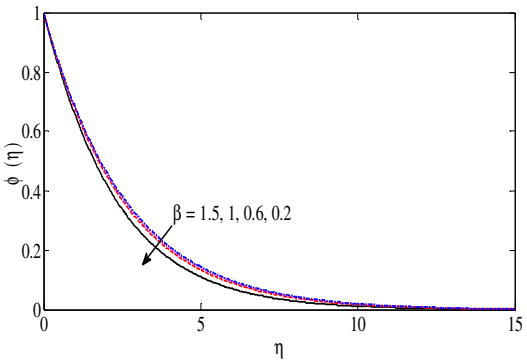

Figure 2c: Dimensionless concentration distribution for different values of β with M = 0.5, Re_x = 1, Gr = 0.2, Gc = 0.2, Fs = 0.1, Da = 0.2, Pr = 2, Q = 0.3, Sc = 0.24, kr = 0.3, λ = 0.4 & f_w = 0.5.

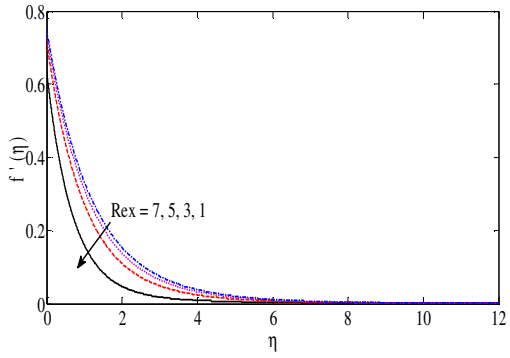

Figure 3a: Dimensionless velocity distribution for different values of $Re_x$with M = 0.5, β = 0.5, Gr = 0.2, Gc = 0.2, Fs = 0.1, Da = 0.2, Pr = 2, Q = 0.3, Sc = 0.24, kr = 0.3, λ = 0.4 & f_w = 0.5.

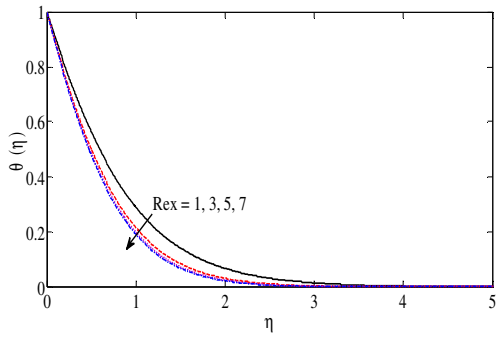

Figure 3b: Dimensionless temperature distribution for different values ofRe_x with M = 0.5, β = 0.5, Gr = 0.2, Gc = 0.2, Fs = 0.1, Da = 0.2, Pr = 2, Q = 0.3, Sc = 0.24, kr = 0.3, λ = 0.4 & f_w = 0.5.

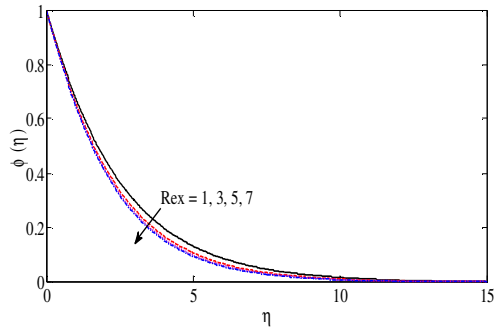

Figure 3c: Dimensionless concentration distribution for different values of Re_x with M = 0.5, β = 0.5, Gr = 0.2, Gc = 0.2, Fs = 0.1, Da = 0.2, Pr = 2, Q = 0.3, Sc = 0.24, kr = 0.3, λ = 0.4 & f_w = 0.5.

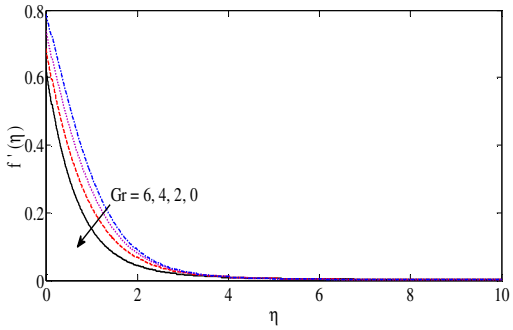

Figure 4a: Dimensionless velocity distribution for different values of*Gr* with M = 0.5, β = 0.5, Re_x = 1, Gc = 0.2, Fs = 0.1, Da = 0.2, Pr = 2, Q = 0.3, Sc = 0.24, kr = 0.3, λ = 0.4 & f_w = 0.5.

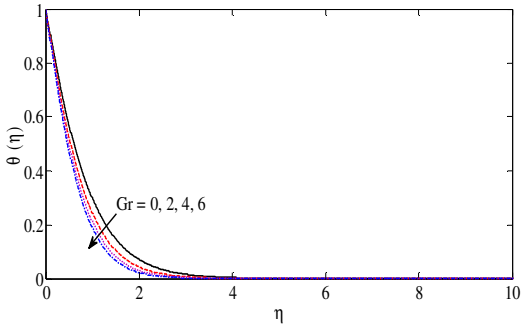

Figure 4b: Dimensionless temperature distribution for different values of *Gr* with M = 0.5, β = 0.5, Re_x = 1, Gc = 0.2, Fs = 0.1, Da = 0.2, Pr = 2, Q = 0.3, Sc = 0.24, kr = 0.3, λ = 0.4 & f_w = 0.5.

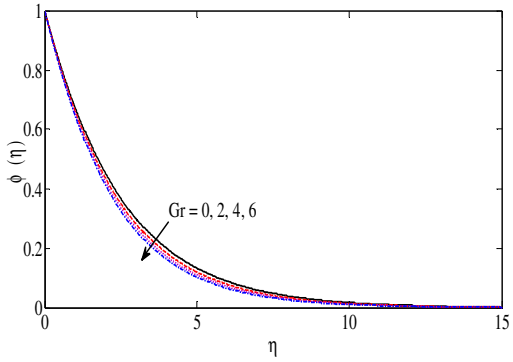

Figure 4c: Dimensionless concentration distribution for different values of *Gr* with M = 0.5, β = 0.5, Re_x = 1, Gc = 0.2, Fs = 0.1, Da = 0.2, Pr = 2, Q = 0.3, Sc = 0.24, kr = 0.3, λ = 0.4 & f_w = 0.5.

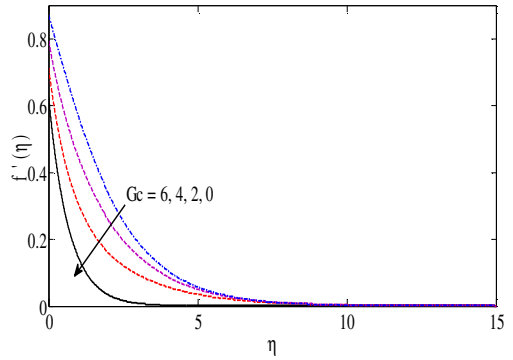

Figure 5a: Dimensionless velocity distribution for different values of *Gc* with M = 0.5, β = 0.5, Re_x = 1, Gr = 0.2, Fs = 0.1, Da = 0.2, Pr = 2, Q = 0.3, Sc = 0.24, kr = 0.3, λ = 0.4 & f_w = 0.5.

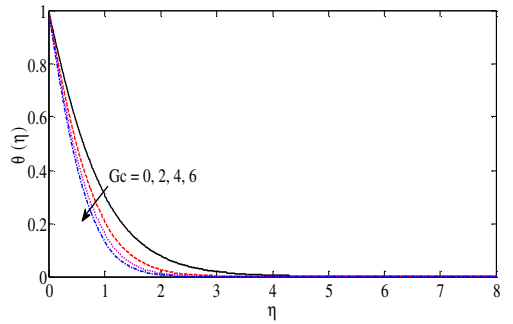

Figure 5b: Dimensionless temperature distribution for different values of *Gc* with M = 0.5, β = 0.5, Re_x = 1, Gr = 0.2, Fs = 0.1, Da = 0.2, Pr = 2, Q = 0.3, Sc = 0.24, kr = 0.3, λ = 0.4 & f_w = 0.5.

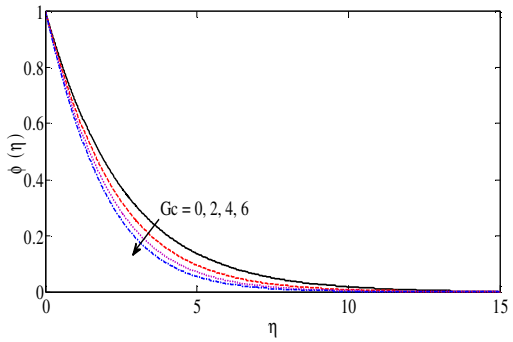

Figure 5c: Dimensionless concentration distribution for different values of *Gc* with M = 0.5, β = 0.5, Re_x = 1, Gr = 0.2, Fs = 0.1, Da = 0.2, Pr = 2, Q = 0.3, Sc = 0.24, kr = 0.3, λ = 0.4 & f_w = 0.5.

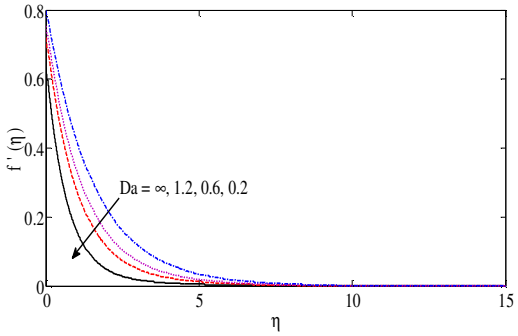

Figure 6a: Dimensionless velocity distribution for different values of *Da* with M = 0.5, β = 0.5, Re_x = 1, Gr = 0.2, Gc = 0.2, Fs = 0.1, Pr = 2, Q = 0.3, Sc = 0.24, kr = 0.3, λ = 0.4 & f_w = 0.5.

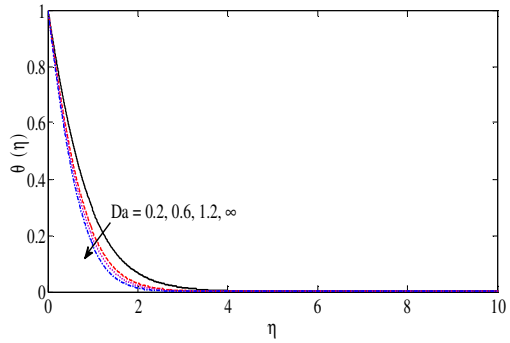

Figure 6b: Dimensionless temperature distribution for different values of *Da* with M = 0.5, β = 0.5, Re_x = 1, Gr = 0.2, Gc = 0.2, Fs = 0.1, Pr = 2, Q = 0.3, Sc = 0.24, kr = 0.3, λ = 0.4 & f_w = 0.5.

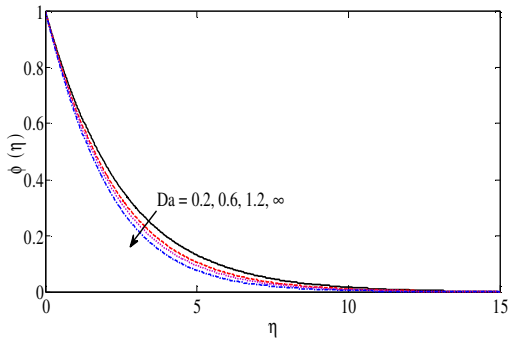

Figure 6c: Dimensionless concentration distribution for different values of *Da* with M = 0.5, β = 0.5, Re_x = 1, Gr = 0.2, Gc = 0.2, Fs = 0.1, Pr = 2, Q = 0.3, Sc = 0.24, kr = 0.3, λ = 0.4 & f_w = 0.5.

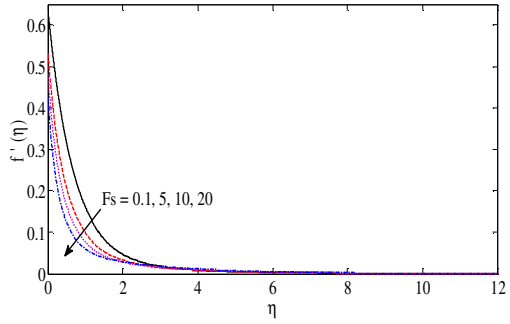

Figure 7a: Dimensionless velocity distribution for different values of *Fs* with M = 0.5, β = 0.5, Re_x = 1, Gr = 0.2, Gc = 0.2, Da = 0.2, Pr = 2, Q = 0.3, Sc = 0.24, kr = 0.3, λ = 0.4 & f_w = 0.5.

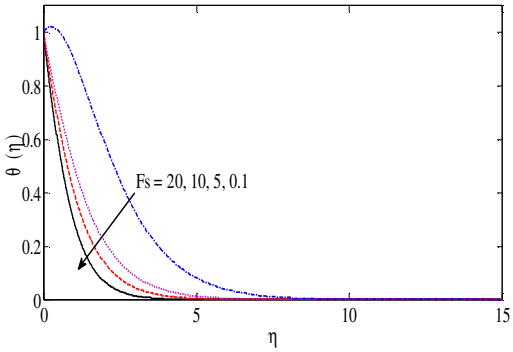

Figure 7b: Dimensionless temperature distribution for different values of *Fs* with M = 0.5, β = 0.5, Re_x = 1, Gr = 0.2, Gc = 0.2, Da = 0.2, Pr = 2, Q = 0.3, Sc = 0.24, kr = 0.3, λ = 0.4 & f_w = 0.5.

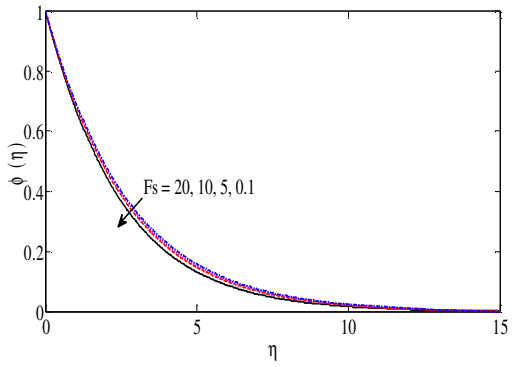

Figure 7c: Dimensionless concentration distribution for different values of *Fs*with M = 0.5, β = 0.5, Re_x = 1, Gr = 0.2, Gc = 0.2, Da = 0.2, Pr = 2, Q = 0.3, Sc = 0.24, kr = 0.3, λ = 0.4 & f_w = 0.5.

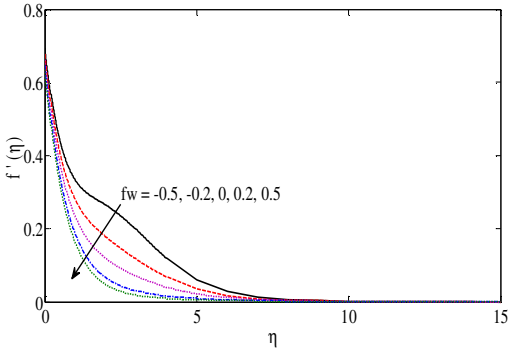

Figure 8a: Dimensionless velocity distribution for different values of f_w for M = 0.5, β = 0.5, Re_x = 1, Gr = 0.2, Gc = 0.2, Fs = 0.1, Da = 0.2, Pr = 2, Q = 0.3, Sc = 0.24, kr = 0.3 & λ = 0.4.

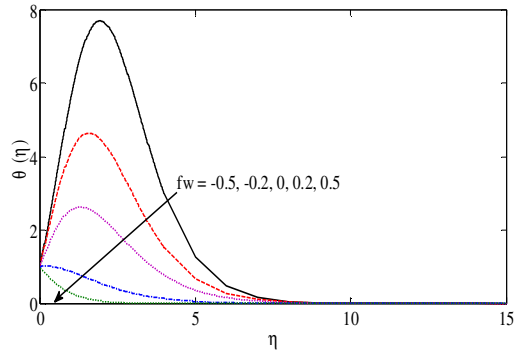

Figure 8b: Dimensionless temperature distribution for different values off$_w$ for M = 0.5, β = 0.5, Re_x = 1, Gr = 0.2, Gc = 0.2, Fs = 0.1, Da = 0.2, Pr = 2, Q = 0.3, Sc = 0.24, kr = 0.3 & λ = 0.4.

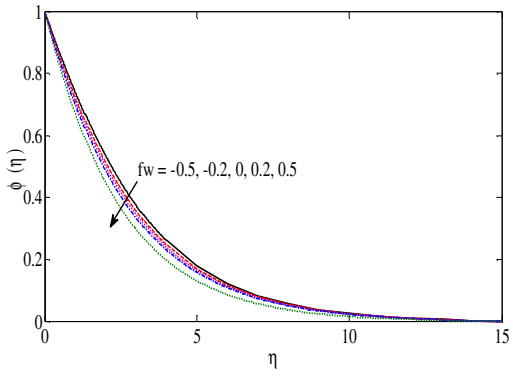

Figure 8c: Dimensionless concentration distribution for different values of f_w forM = 0.5, β = 0.5, Re_x = 1, Gr = 0.2, Gc = 0.2, Fs = 0.1, Da = 0.2, Pr = 2, Q = 0.3, Sc = 0.24, kr = 0.3 & λ = 0.4.

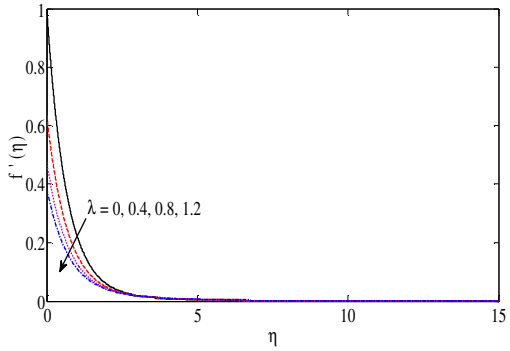

Figure 9a: Dimensionless velocity distribution for different values of λ with M = 0.5, β = 0.5, Re_x = 1, Gr = 0.2, Gc = 0.2, Fs = 0.1, Da = 0.2, Pr = 2, Q = 0.3, Sc = 0.24, kr = 0.3 & f_w = 0.5.

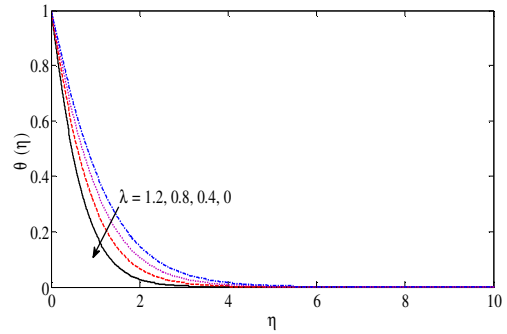

Figure 9b Dimensionless temperature distribution for different values of λ with M = 0.5, β = 0.5, Re_x = 1, Gr = 0.2, Gc = 0.2, Fs = 0.1, Da = 0.2, Pr = 2, Q = 0.3, Sc = 0.24, kr = 0.3 & f_w = 0.5.

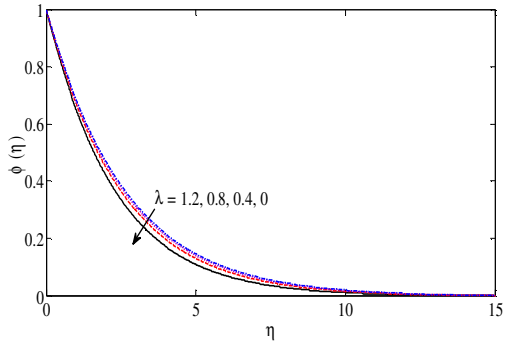

Figure 9c: Dimensionless concentration distribution for different values of λ with M = 0.5, β = 0.5, Re_x = 1, Gr = 0.2, Gc = 0.2, Fs = 0.1, Da = 0.2, Pr = 2, Q = 0.3, Sc = 0.24, kr = 0.3& f_w = 0.5.

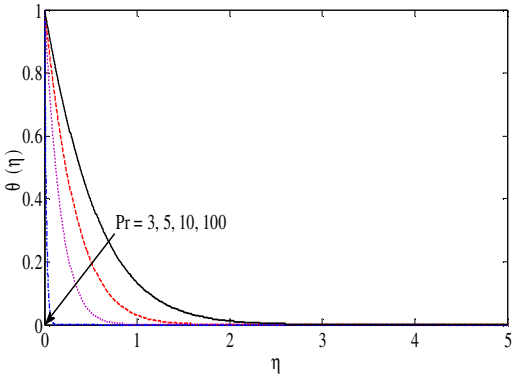

Figure 10: Dimensionless temperature distribution for different values of Pr with M = 0.5, β = 0.5, Re_x = 1, Gr = 0.2, Gc = 0.2, Fs = 0.1, Da = 0.2, Q = 0.3, Sc = 0.24, kr = 0.3, λ = 0.4 & f_w = 0.5.

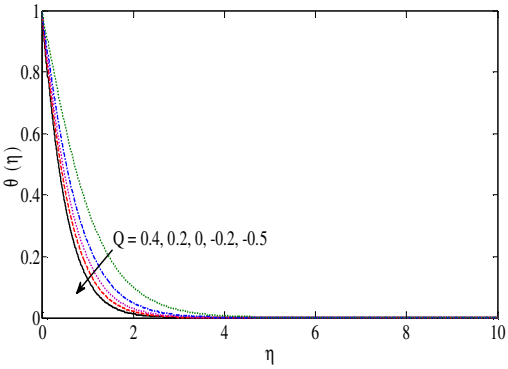

Figure 11: Dimensionless temperature distribution for different values of Q with M = 0.5, β = 0.5, Re_x = 1, Gr = 0.2, Gc = 0.2, Fs = 0.1, Da = 0.2, Pr = 2, Sc = 0.24, kr = 0.3, λ = 0.4 & f_w = 0.5.

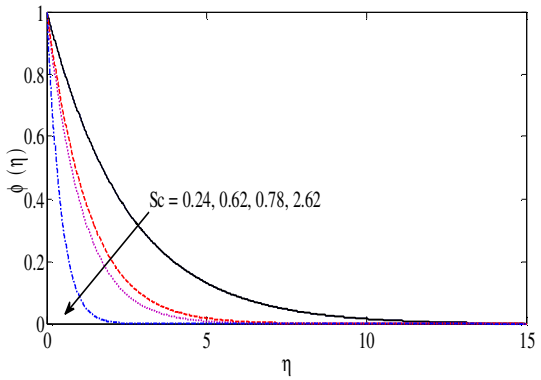

Figure 12: Dimensionless concentration distribution for different values of Sc with M = 0.5, β = 0.5, Re_x = 1, Gr = 0.2, Gc = 0.2, Fs = 0.1, Da = 0.2, Pr = 2, Q = 0.3, Sc = 0.24, kr = 0.3, λ = 0.4 & f_w = 0.5.

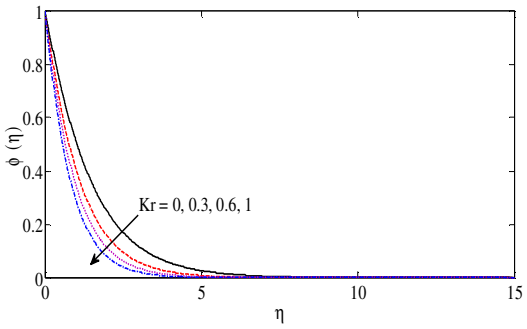

Figure 13: Dimensionless concentration distribution for different values of kr with M = 0.5, β = 0.5, Re_x = 1, Gr = 0.2, Gc = 0.2, Fs = 0.1, Da = 0.2, Pr = 2, Q = 0.3, Sc = 0.24, kr = 0.3, λ = 0.4 & f_w = 0.5.

REFERENCES

1. Abbas Z., Javed T., Ali N., and Sajid M., (2016), Diffusion of Chemically Reactive species in stagnation –point flow of a third grade fluid: a Hybrid Numerical Method, Journal of Applied Fluid Mechanics, Vol.9, No.1, pp.195-203.
2. Ali J Chamkha, Sameh E. Ahmed and Abdulkareem S. Aloraier, (2010), Melting and radiation effects on mixed convection from a vertical surface embedded in a non-Newtonian fluid saturated non-Darcy porous medium for aiding and opposing eternal flows, International Journal of the Physical Sciences, Vol.5 (7), pp.1212-1224.
3. Aly E.H., Eliott L. and lngham D.B., (2003), Mixed convection boundary layer flow over a vertical surface embedded in a porous medium, European Journal of Mechanics-B/Fluids, Vol. 22, pp.529-543.

4. Anderson H.I., Hansen O.R. and Holmedal B., (1994), Diffusion of Chemically Reactive Species from a Stretching Sheet, International Journal of Heat and Mass Transfer, Vol.37, pp.659-664.
5. Eldabe N.T.M. and Salwa M.G.E., (1995), Heat Transfer of MHD Non-Newtonian Casson Fluid Flow between two Rotating Cylinders, Journal of the Physical Society of Japan, Vol.64, 41.
6. Emmanuel Maurice Arthur, Ibrahim Yakubu Seini, Letis Bortey Bortteir, (2015), Analysis of Casson Fluid Flow over a Vertical Porous Surface with Chemical Reaction in the Presence of Magnetic Field, Journal of Applied Mathematics and Physics, Vol.3, pp.713-723.
7. Fazlina Aman and Ansur Ishak, (2012), Mixed Convective Boundary Layer Flow towards aVertical Plate with a Convective surface boundary Condition, Hindawi Publishing Corporation Mathematical Problems in Engineering, Vol. 2012, 11 pages doi:1155/2012/453457
8. Gangadhar K., Bhaskar reddy N,, Kameswaran P. K., (2012), Similarity solution of HydroMagnetic Heat and Mass Transfer over a Vertical plate with a convective surface boundary condition and Chemical Reaction, International journal of Nonlinear science, Vol.13, No.3, pp.298-307.
9. Hayat T., Muhammad T., Shehzad S.A., Alsaedi A., (2015), Temperature and Concentration Stratification Effects in Mixed Convection Flow of an Oldroyd-B Fluid with Thermal Radiation and Chemical Reaction, PLOS ONE, Vol.10 (6) :e0127646 doi:10.137/journal.pone.127646
10. Krishnendu Bhattacharya, Swati mukhopadhyay, Layek G.C., (2013), Similarity solution of mixed convective boundary layer slip flow over a vertical plate, Ain Shams Engineering Journal, Vol.4, pp.299-305.
11. Mahammed Jashmin Uddin, Osman Anwar Beg, and Ahmad Izani Md. Ismail, Mathematical Modelling of Radiative Hydromagnetic Thermosolutal Nanofluid Convection slip Flow in Saturated Porous Media, Hindawi Publishing Corporation Mathematical Problems in Engineering, Vol.2014, 11 pages, http://dx.doi.org/1155/2014/179172
12. Mahdy A., Rama Subba Reddy Gorla, (2014), Soret and Dufour effects on MHD non-Darcian natural convection from a vertical wavy surface embedded in a porous medium, Thermal Energy and Powe Engineering, TEPE, Vol. 3, pp.206-215.
13. Murthy R.V.S.N. and Singh P., (2000), Thermal Dispersion Effects on non-Darcy convection over a cone, An International Journal Computers and Mathematics with Applications, Vol.40, pp.1433-1444.
14. Mythili D., Sivaraj R, Rashidi M.M. and Yang Z., (2015), Casson fluid flow over a vertical cone with non-uniform heat source/sink and high order chemical reaction, Journal of Naval Architecture and Marine Engineering, Vol.15, pp.125-136.
15. Norfifah Bachok, Anuar Ishak and loan pop, (2010), Mixed Convection Boundary Layer Flow over a Permeable Vertical Flat Plate Embedded in an isotropic Porous Medium, Hindawi Publishing Corporation Mathematical Problems in Engineering, Vol.2010, 12 pages, doi:10.1155/2010/659023.

16. Ralston, Wilf, (1960), Mathematical Methods for Digital Computers, John Wiley and Sons, N.Y., 117.
17. Rama Subba Reddy Gorla and Ali Chamkha, (2011), Natural convective boundary layer flow over a non isothermal vertical plate embedded in a porous medium saturated with a nanofluid, Nanoscale and Microscale Thermophysical Engineering, Vol.15, pp.81-94.
18. Sachin Shaw, Peri K Kameswaran and Precious Sibanda, (2016), Effects of slip on nonlinear convection in nanofluid flow on stretching surfaces, Boundary value Problems, Vol.2016:2, DOI 10.1186/s13661-015-0506-2.
19. Saida siddiqa and Hossain M. A., (2012), Mixed convection boundary layer flow over a vertical flat plate with radiative heat transfer, Applied Mathematics, Vol.3, pp.705-716.
20. Saida Siddiqa, Hossain M.A., (2012), Mixed Convection Boundary Layer Flow over a Vertical Flat plate with Radiative Heat Transfer Applied Mathematics, Vol.3, pp.705-716.
21. Salem A.M. and EI-Aziz M.A., (2008), Effect of Hall Currents and Chemical Reaction on Hydromagnetic Flow of a Stretching Vertical Surface with Internal Heat Generation/Absorption, Applied Mathematical Modelling, Vol.32, pp.1236-1254.
22. Seth G. S., Sharma R. and Kumbhakar B., (2016), Heat and Mass Transfer effects on unsteady MHD Natural convection flow a chemically reactive and radiating fluid through a porous medium past a moving vertical plate with arbitrary ramped temperature, Journal of Applied Fluid Mechanics, Vol.9, pp.103-117.
23. Shezad S.A., Hayat T., and Alsaedi A., (2016), Three –Dimensional MHD flow of Casson fluid in porous medium with heat generation, Journal of Applied Fluid Mechanics, Vol.9, No.1, pp.215-223.
24. Shezad S.A., Hayat T., Qasim M., and asghar S., (2013), Effects of Mass Transfer on MHD Flow of Casson Fluid with Chemical Reaction and Suction, Brazilian Journal of Chemical Engineering, Vol.30, pp.187-195.
25. Siva Ram Prasad J., and Hemalatha K., (2016), A study on mixed convective MHD flow from a vertical plate embedded in non-Darcy porous medium with melting effect, Journal of Applied Fluid Mechanics, Vol.9, No.1, pp.293-302.
26. Srinivasacharya D., and Poshala Vijay Kumar P., (2015), Mixed convection over an inclined wavy surface in a nanofluid saturated Non-Darcy Porous medium with Radiation Effect, Hindavi Publishing Corporation, International Journal of Chemical Engineering, Vol.2015, 15 pages http://dx.doi.org/10.1155/2015/927508.
27. Subbarao Annasagaram, PrasadVallampati R., Bhaskar Reddy Nandanoor and Anwer Beg Osman, (2015), Modelling laminar transport phenomena in a Casson rheological fluid from an isothermal sphere with partial slip, Thermal science, Vol.19, pp.15407-1519.